Colloid Polym Sci (2013) 291:1525–1534
DOI 10.1007/s00396-012-2873-x

SHORT COMMUNICATION

Synthesize procedures, mechanical and thermal properties of thiazole bearing poly(amid-imide) composite thin films containing multiwalled carbon nanotubes

Shadpour Mallakpour · Amin Zadehnazari

Received: 9 October 2012 / Revised: 22 November 2012 / Accepted: 27 November 2012 / Published online: 12 December 2012

Abstract This research is aimed at characterizing the thermal, mechanical, and morphological properties of carbon nanotubes (CNTs) reinforced poly(amide-imide) (PAI) composites having thiazol and amino acid groups which were prepared by sonication-assisted solution compounding. To increase the compatibility between the PAI matrix and CNTs, carboxyl-functionalized multiwall CNTs (MWCNTs-COOH) were used in this study. The MWCNTs were dispersed homogeneously in the PAI matrix while the structure of the polymer and the MWCNTs structure are stable in the preparation process as revealed by transmission electron microscopy. MWCNT/PAI composite films have been prepared by casting a solution of precursor polymer containing MWCNTs into a thin film, and its tensile properties were examined. The thermal stability, Young's modulus, and tensile strength of PAI were greatly improved by the incorporation of MWCNTs and their good dispersion. Composites were also characterized by Fourier transform infrared spectroscopy, X-ray diffraction, scanning electron microscopy, and thermal gravimetric analysis.

S. Mallakpour (✉) · A. Zadehnazari
Organic Polymer Chemistry Research Laboratory, Department of Chemistry, Isfahan University of Technology, Isfahan 84156-83111, Islamic Republic of Iran
e-mail: mallak@cc.iut.ac.ir

S. Mallakpour
e-mail: mallak777@yahoo.com

S. Mallakpour
e-mail: mallakpour84@alumni.ufl.edu

S. Mallakpour
Nanotechnology and Advanced Materials Institute, Isfahan University of Technology, Isfahan 84156-83111, Islamic Republic of Iran

Keywords Carbon nanotubes · Ultrasonics · Polymer-matrix composites · Mechanical testing · Thermogravimetric analysis

Introduction

Carbon nanotubes (CNTs) were shown in the last years as attractive fillers for polymers in order to improve mechanical strength, reach conductivity at low loadings, influence the thermal stability, thermal expansion, wear and friction behavior favorably. This is due to their extremely high aspect ratio and low density as well as their fiber-like shape [1, 2]. Recently, there has been an increasing attention in the studies of CNT/polymer composites due to the unique combination of promising properties and construction of multifunctional structures of each component. These composites exhibit potentially superior the thermal, electrical, and mechanical properties than the pristine polymers [3, 4]. It is well recognized that the properties of polymeric materials are highly affected by nano-sized fillers incorporated into the polymer matrix, which are highly dependent on the type and the dimension of fillers, their dispersion state, and the interaction with the polymer matrix [5]. CNTs, however, have rarely been used as mechanical or electrical inclusions in a polymer matrix because of the difficulty in achieving efficient dispersion. This difficulty is primarily due to attractive van der Waal's forces between carbon surfaces. CNTs tend to aggregate together inside the solution and form ropes, usually with highly entangled network structures [6]. But, by careful procedure, we can blend these two components without severe aggregation of CNTs. The attractive forces also arise due to an entropic effect inside the polymer matrix [7]. Polymer chains in the region of the colloidal filler suffer an entropic penalty since roughly half of their configurations are precluded. Therefore, there is a depletion of the polymer in this region, resulting in an

osmotic pressure forcing the filler particles to come together. To overcome the difficulty of dispersion, several mechanical/physical methods such as ultrasonication and chemical modification through functionalization are already reported [8–12]. These methods are mainly based on the noncovalent interactions including π–π stacking, van der Waals or charge transfer interactions [13–15], covalent (grafting-to and grafting-from) [16–20], and adsorption of surfactants [21]. In general, all of these different techniques give various results in terms of the efficiency of the nanotubes dispersion, interfacial interaction between components, properties of the composites, and possible promising applications.

Polyimides are well recognized as a class of high-performance polymers due to their resistance to high temperatures, mechanical stress, and a variety of chemicals [22]. However, the intractable characteristics have been major problems as a result of high melting point and insolubility. To overcome this problem, various copolyimides and polymer structure modification have been developed. For example, poly(amide-imide)s (PAIs) have been developed as an alternative material offering a compromise between excellent thermal stability and processability. They can be synthesized by two well-established methods: the reaction of diimide dicarboxylic acids with diamines in the presence of triphenyl phosphite (TPP) and metallic salts, as condensing agent, or by the reaction of diacid chlorides with diamines in the presence of an acid acceptor by classical way or by microwave irradiation [23–25].

In recent years, the effect of adding nanofillers on the physical and mechanical properties of PAIs has been studied by many groups, but a few studies concerned with the fabrication of multi walled-CNT (MWCNT)/PAI composites have been carried out [26–28]. A number of researchers have undertaken covalent stabilization techniques to molecularly bind (or to functionalize) specific molecular species onto CNT surfaces for enhanced dispersion and functionality [16–20]; however, a noncovalent approach via hydrogen interaction of MWCNTs-COOH in polymer solution is selected for this study as this method preserves the mechanical and physical properties of individual CNTs. A small number of studies have also been focused on improving the dispersion of CNTs via the synthesis of polymer with several functional and bulky pendent groups for the matrix polymer itself. In this study, a simple ultrasonication-assisted solution blending process for fabricating composites and a casting method for the preparation of composite films is proposed in order to study the certain properties of the resulting composites, including thermal and tensile mechanical properties. The introduction of several functional groups as well as thiazol and amino acid bulky substituents resulted in increased chain packing distances and decreased intermolecular interactions, leading to better interaction of the PAI chains with MWCNTs-COOH and better dispersion of MWCNTs in the PAI matrix.

Experimental

Reagents and materials

All chemicals used in this study were obtained commercially from Fluka Chemical Co. (Switzerland), Aldrich Chemical Co. (Milwaukee, WI), and Merck Chemical Co. (Germany). 2-Aminothiazole, 3,5-dinitrobenzoylchloride, acetone, hydrazine hydrate, $FeCl_3$, and propylene oxide from Merck were used for the synthesis of mediators. Propylene oxide was used as acid scavenger. *N,N′*-dimethylformamide (DMF) (d=0.94 gcm^{-3} at 20 °C) and *N,N′*-dimethylacetamide (DMAc) as solvent (d=0.94 gcm^{-3} at 20 °C) were distilled over barium oxide under reduced pressure. Carboxyl-modified MWCNT (purity >95 % and carboxyl content 2.56 wt.%) used in this study, purchased from Neutrino Co. (Iran), have outer diameters of 8–15 nm and lengths of ~50 μm. Other reagents were used without further purification.

Characterization and instrumentation

The apparatus used for the step-growth polymerization reaction was a Samsung microwave oven (2,450 MHz, 900 W) (Korea). Fourier transform infrared (FT-IR) spectra of the composite films were recorded with a Jasco-680 (Japan) spectrometer at a resolution of 4 cm^{-1}, and they were scanned at wave number range of 400–4,000 cm^{-1}. Band intensities are assigned as weak (w), medium (m), strong (s), and broad (br). Vibration bands were reported as wave number (cm^{-1}). ^{1}H and ^{13}C nuclear magnetic resonance (NMR) spectra were recorded on a Bruker (Germany) Avance 500 instrument at room temperature in dimethylsulphoxide-d_6 (DMSO-d_6). Multiplicities of proton resonance were designated as singlet (s), doublet (d), triplet (t), and multiplet (m). ^{13}C spectrum is broadband proton decoupled. The chemical shifts were reported in parts per million with respect to the references and were stated relative to external tetramethylsilane for ^{1}H and ^{13}C NMR. Elemental analysis was performed in an Elementar Analysensysteme GmbH (Germany). Inherent viscosity was measured by using a Cannon Fenske Routine Viscometer (Germany) at the concentration of 0.5 g/dL in DMF at 25 °C. Optical specific rotation was measured at concentration of 0.5 g/dL in DMF at 25 °C using a quartz cell (1.0 cm) with a Jasco Polarimeter (JASCO Co., Ltd., Japan). Thermal stability of the MWCNT/PAI composites was evaluated by recording thermogravimetric analysis (TGA)/derivative thermogravimetric (DTG) traces (STA503 win TA TGA,

Germany) in nitrogen atmosphere (flow rate 60 cm^3/min). A heating rate of 10 °C/min and a sample size of 10±2 mg were used in each experiment. The X-ray diffraction (XRD) was used to characterize the crystalline structure of the composites. XRD patterns were collected using a Bruker, D8ADVANCE (Germany) diffractometer with a copper target at the wave length of λ Cu Kα=1.54 Å, a tube voltage of 40 kV, and tube current of 35 mA. The samples were scanned at a rate of 0.05°/min from 10° to 80° of 2θ. For XRD studies, rectangular pellets prepared by compression molding were used. The dispersion morphology of the MWCNTs in the PAI matrix was observed using field emission scanning electron microscopy (FE-SEM, HITACHI S-4160, Japan). Transmission electron microscopy (TEM) micrographs were obtained using a Philips CM 120 (Germany) microscope with an accelerating voltage of 100 kV. For TEM studies, ultra-thin sections (30–80 nm) of the composites were prepared using Leica Ultramicrotome. Tensile testing was performed at room temperature on a Testometric Universal Testing Machine M350/500 (UK), according to ASTM D 882 (standards). Tests were carried out with a cross-head speed of 12.5 mm/min until/to a deformation of 20 % and then at a speed of 50 mm/min at break. The dimensions of the test specimens were 35×2×0.04 mm^3. Tensile strength, tensile modulus, and strain were obtained from these measurements. Preparation of the MWCNT/PAI composites was carried out on a MISONIX ultrasonic XL-2000 SERIES, USA. Ultrasonic irradiation was performed with the probe of the ultrasonic horn immersed directly in the mixture solution system with frequency 2.25×10^4 Hz and power 100 W.

Monomer synthesis

Synthesis of 3,5-diamino-N-(thiazol-2-yl)benzamide (4)

Iron oxide hydroxide catalyst was prepared according to the literature [29]. 3,5-Dinitro-*N*-(thiazol-2-yl)benzamide (3) was also prepared according to the reported procedure [30]. To a suspension of the purified 3,5-dinitro-*N*-(thiazol-2-yl)benzamide (1.0 g, 3.4 mmol) and iron oxide hydroxide (0.1 g, 1.13 mmol) in methanol (15 mL), hydrazine monohydrate (1.5 mL) was added dropwise to the stirred mixture at 60 °C within 10 min. After complete addition, the mixture was heated at the reflux temperature for another 12 h. The reaction solution was filtered hot to remove iron oxide hydroxide, and the filtrate was then filtered cold to remove the solvent. The crude product was purified by recrystallization from methanol to give 0.68 g of diamine 4 as brown needles (68 % yield, m.p. = 208–210 °C) [31].

FT-IR (KBr; cm^{-1}): 3,434 (s, N–H stretch), 3,385 (s, N–H stretch), 3,103 (w, C–H aromatic), 1,662 (s, C=O amide stretch), 1,560 (m), 1,525 (m) 1,459 (w), 1,326 (w), 1,161 (w, C–O stretch), 830 (m), 779 (w, N–H out-of-plane bending). ^{1}H NMR (DMSO-d_6; δ, ppm): 4.907 (s, 4 H, NH), 6.060 (s, 1 H, Ar–H), 6.454 (s, 2 H, Ar–H), 7.199–7.208 (d, 1 H, Ar–H, J=3.60 Hz), 7.449–7.507 (d, 1 H, Ar–H, J=3.20 Hz), 11.823 (s, 1 H, NH). ^{13}C NMR (DMSO-d_6; δ, ppm): 102.55 (CH, Ar), 103.01 (CH, Ar), 113.39 (CH, thiazole ring), 133.61 (C, Ar), 137.66 (CH, thiazole ring), 149.20 (C, Ar), 158.57 (C, Ar), 166.45 (C, C=O). Elemental analysis: calculated for $C_{10}H_{10}N_4OS$: C, 51.27 %; H, 4.30 %; N, 23.91 %; S, 13.69 %; found: C, 51.40 %; H, 4.330 %; N, 23.87 %; S, 13.54 %.

Synthesis of N-trimellitylimido-S-valine (2)

N-trimellitylimido-*S*-valine (5) was prepared according to our previous work [32].

Synthesis of PAI

A mixture of 0.10 g (0.34 mmol) of *N*-trimellitylimido-*S*-valine (5), 0.08 g (0.34 mmol) of diamine 4, and 0.44 g of tetrabutylammonium bromide (TBAB) (1.36 mmol) were placed in a porcelain dish and was ground completely for 5 min, then 0.23 mL (1.36 mmol) of TPP was added, and the mixture was ground for 3 min. The reaction mixture was irradiated in the microwave oven for 240 s at 100 % of power level (900 W). The resulting viscous solution was poured into 30 mL of methanol, filtered, and dried at 80 °C for 6 h under vacuum to give 0.17 g (94 %) of yellow powder PAI6. The optical specific rotation was measured ($[\alpha]^{25,b}_{Na,589}$= −32.29) at a concentration of 0.5 g/dL in DMF at 25 °C. The inherent viscosity was also measured (η_{inh}=0.48 dL/g) under similar conditions.

FT-IR (KBr, cm^{-1}): 3,454 (m, br, N–H stretch), 3,101 (w, C–H aromatic), 2,925 (w, C–H aliphatic), 1,776 (m, C=O imide, asymmetric stretching), 1,719 (s, C=O imide, symmetric stretching), 1,671 (m, C=O amide, stretching), 1,602 (s), 1,546 (m), 1,450 (s), 1,376 (m, CNC axial stretching), 1,201 (m, CNC transverse stretching), 1,069 (m), 725 (s, CNC out-of-plane bending), 619 (w). ^{1}H NMR (DMSO-d_6; δ, ppm): 0.99 (d, 3 H, CH_3, distorted), 1.01 (d, 3 H, CH_3, distorted), 2.84 (m, 1 H, CH), 4.64-4.66 (d, 1 H, CH, J=7.6 Hz), 7.26 (s, 1 H, Ar-H), 7.54 (s, 1 H, Ar-H), 7.91 (s, 1 H, Ar-H), 7.96 (d, 1 H, Ar-H, distorted), 8.10 (d, 1 H, Ar-H, distorted), 8.28 (d, 1 H, Ar-H, distorted), 8.44 (d, 1 H, Ar-H, distorted), 8.52 (s, 1 H, Ar-H), 10.31 (s, 1 H, NH), 10.92 (s, 2 H, NH), 12.73 (s, H, NH). Elemental analysis: calculated for $(C_{24}H_{19}N_5O_5S)_n$: C, 58.90 %; H, 3.91 %; N, 14.31 %; S, 6.55 %. Found: C, 59.12 %; H, 3.47 %; N, 14.09 %; S, 6.23 %.

Preparation of the MWCNT/PAI composite films

To attain uniformly mixed MWCNT/PAI solutions with desired weight percentages of MWCNT, a two-step method

was used. First, two stock solutions were prepared: PAI was dissolved and MWCNTs were separately dispersed in DMAc solution with stirring for 1 day at 30–40 °C. Then, two stock solutions were mixed to achieve the desired weight percentages of MWCNTs from 5 to 15 wt.%. The MWCNT/PAI solutions were stirred for 1 day at 30–40 °C and then ultrasonicated in water bath for 1 h. To remove the DMAc solvent, MWCNT/PAI solutions were poured into uncovered preheated glass Petri dishes and uniformly heated at 60 °C for 1 day; then the semidried film was further dried in vacuo at 160 °C for 8 h to remove the residual solvent, and a solid film was formed. Curly films formed after evaporation of DMAc, and could be easily lifted from the glass Petri dishes. Freestanding polymer films 30–40-μm thick were then peeled from the glass plate and were subjected to different tests. Because MWCNTs are black in color, the films containing more MWCNTs look darker: film colors varied from tan (0 % MWCNT) to light gray (5 % MWCNT) to dark black (10 and 15 % MWCNT). Uniform color was observed, an indication of good distribution of MWCNTs in the polymer matrix.

Results and discussion

Synthesis and structural characterization of monomers

Diacid monomer was synthesized by the condensation reaction of an equimolar amount of trimellitic anhydride and *S*-valine amino acid in the reflux acetic acid solution [32]. Scheme 1 (upside) shows the synthetic route to 3,5-diamino-*N*-(thiazol-2-yl)benzamide by a two-step process. In the first step, nucleophilic displacement of 2-aminothiazole with 3,5-dinitrobenzoylchloride in acetone solvent resulted in 3,5-dinitro-*N*-(thiazol-2-yl)benzamide as a pale yellow solid [30]. In the second step, this dinitro compound was reduced in methanol in the presence of hydrazine hydrate and a catalytic amount of iron oxide hydroxide at 60 °C to produce brown crystals of the diamine 4. The structure of the diamine 4 was identified by elemental analysis, FT-IR, and NMR spectroscopic methods. In the FT-IR spectrum of diamine 4, the peak attributed to the stretching vibration of the bond C=O appeared at 1,662 cm^{-1}. The absorption peaks of amine functions are obvious as two peaks at 3,434 and 3,385 cm^{-1}. In the ^{1}H NMR spectrum of diamine 4, the signals of aromatic protons appear in the range of 6.060–7.507 ppm, and the characteristic resonance signal at 4.907 ppm is due to the amino group. Moreover, the proton for the amide group is observed at 11.823 ppm. Furthermore, in the ^{13}C NMR spectrum, seven peaks corresponding to the seven kinds of aromatic carbons appeared in the range of 102.55–158.57 ppm. This spectrum also exhibited a peak for carbonyl of amide group at 166.45 ppm.

Synthesis of PAI

In the course of our study on the application of green chemistry principles in polymerization [33, 34], we wish to report a fast, simple, safe, and efficient method for the step-growth polymerization of natural S-valine-based diacid 5 with an aromatic thiazole-based diamine (4) in the molten TBAB in the presence of TPP under microwave irradiation. Scheme 1 (underside) shows the polycondensation reaction to PAI. The effect of microwave power levels and period of heating was examined to provide the optimum reaction conditions. A series of experiments which were performed with different reaction times under microwave irradiations revealed that the optimal results were obtained after 240 s at 100 % of power level. At higher radiation times, dark product was obtained, and on the other hand, under low radiation times, reaction gave low yield and inherent viscosity. This problem could be explained by the fact that molten salts are highly polar media and likely to be strongly microwave absorbing. The inherent viscosity of the synthesized PAI was 0.48 dL/g and the yield was 94 %. The resulting polymer showed optical rotation, which indicated that, the polymer is optically active and chirality was introduced into the backbone of the polymer. The optical specific rotation of this polymer was $[\alpha]^{25,b}_{Na,589} = -32.29$ (0.05 g in 10 mL of DMF). The structure of this polymer was confirmed as PAI using FT-IR spectroscopy, ^{1}H NMR, and elemental analysis techniques.

Fabrication of the composite films

The dispersion of the carboxyl-modified MWCNTs in the 5, 10, and 15 wt.% solutions of PAI in DMAc was achieved by a vigorous stirring with a speed of 15,000 rpm for 1 day using a homogenizer, followed by ultrasonication process for 1 h to form a new series of chiral composites. The reaction pathways for preparing MWCNT/PAI composites are shown in Scheme 2. The effective use of CNTs in composite applications depends on the ability to disperse the CNTs uniformly throughout the matrix without reducing their aspect ratio. Due to the van der Waals attraction, CNTs are held together as bundles and ropes. Therefore, they have very low solubility in solvents and tend to remain as entangled agglomerates. To employ CNTs as effective reinforcement in polymer composites, proper dispersion and appropriate interfacial adhesion between the CNTs and polymer matrix, several mechanical/physical methods were used [8–12]. So, carboxylated MWCNTs were used in this study. The lower level of aggregation in the modified CNTs can be attributed to the presence of functional groups such as carboxyl groups. This transformation should contribute positively to the good dispersion of CNTs in the PAI matrix.

Scheme 1 Synthesis of diamine monomer 4 and PAI6

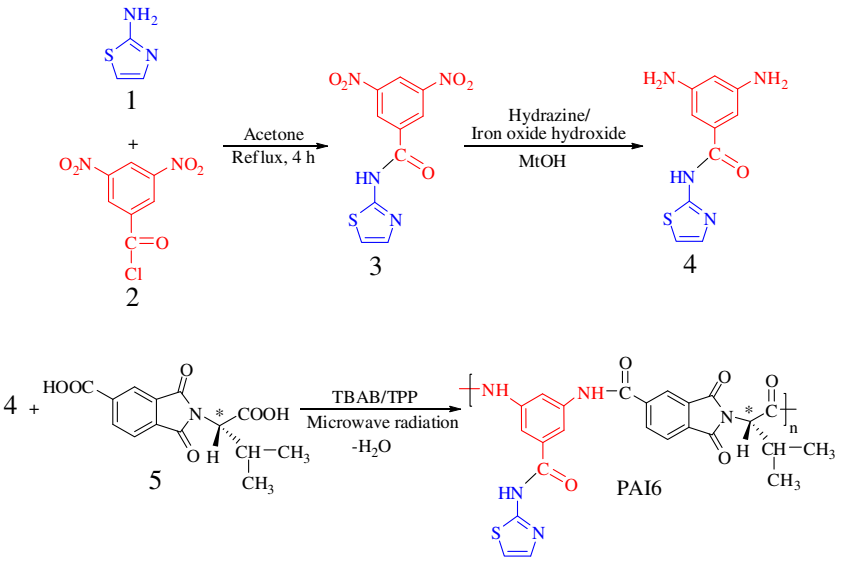

Moreover, the introduction of several functional groups into the matrix of aromatic polymer performs a hydrogen interaction with modified CNTs, and a composite based on hydrogen interaction, by which the PAI chains were tightly attached to the surface of MWCNT-COOH, can be a result. The interaction between PAI chains and MWCNTs-COOH was described in Fig. 1.

Characterization of the composites

Spectral data

The formation of PAI was confirmed using FT-IR spectroscopy. Strong absorption bands were observed at 1,719–1,776 cm^{-1}. These are attributed to the asymmetric and symmetric stretching vibrations of the imide carbonyl groups. The bands of C–N bond stretching and ring deformation appear at 1,376 and 725 cm^{-1}. Strong bands of absorption characteristic for the new formed amide linkage appeared at around 3,454 cm^{-1} assigned to N–H stretching vibration, at 1,671 cm^{-1} attributed to C=O stretching vibration, and at 1,546 cm^{-1} due to N–H bending vibration. The absorption band at around 3,101 cm^{-1} was attributed to = CH aromatic linkage. The aliphatic C–H stretching peak was also appeared at around 2,925 cm^{-1}. The functionalized MWCNTs were also characterized by FT-IR. The spectrum of a pristine MWCNTs/KBr pellet showed a strong, broad absorption band centered at 3,433 cm^{-1}, which is attributed to the O–H stretching bands of carboxylic acid moieties from the surface of MWCNTs. The small peak around 2,923 cm^{-1} was ascribed to aliphatic sp^3 C–H of MWCNTs [35]. The presence of CNTs in the polymer matrix showed very little changes in the FT-IR spectrum, presumably due to the low MWCNT composition and the weak vibration signals of MWCNTs. The structure of neat PAI was also confirmed with ^{1}H NMR spectroscopy. In the ^{1}H NMR spectrum of this polymer, appearances of the N–H protons of amide groups at 10.31, 10.92, and 12.73 ppm, as three singlet peaks, indicate the presence of amide groups in the polymer's structure. The resonance of aromatic protons appeared in the range of 7.26–8.52 ppm. Also, the proton of the chiral center appeared as doublet at 4.64–4.66 ppm.

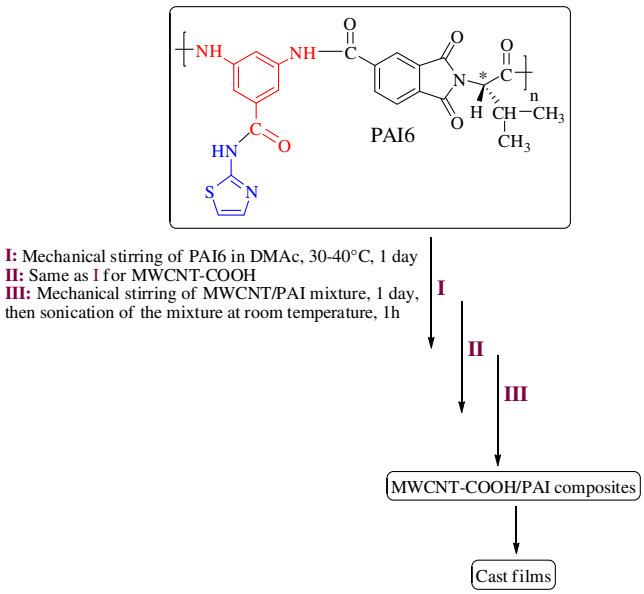

Scheme 2 Schematic of the preparation process of MWCNT/PAI composites

XRD analysis

The structure of the MWCNT/PAI composites was examined by XRD, and the resultant curves are shown in Fig. 2. MWCNTs and pristine PAI were also investigated and compared. For the MWCNTs, two peaks appeared at 2θ=26°

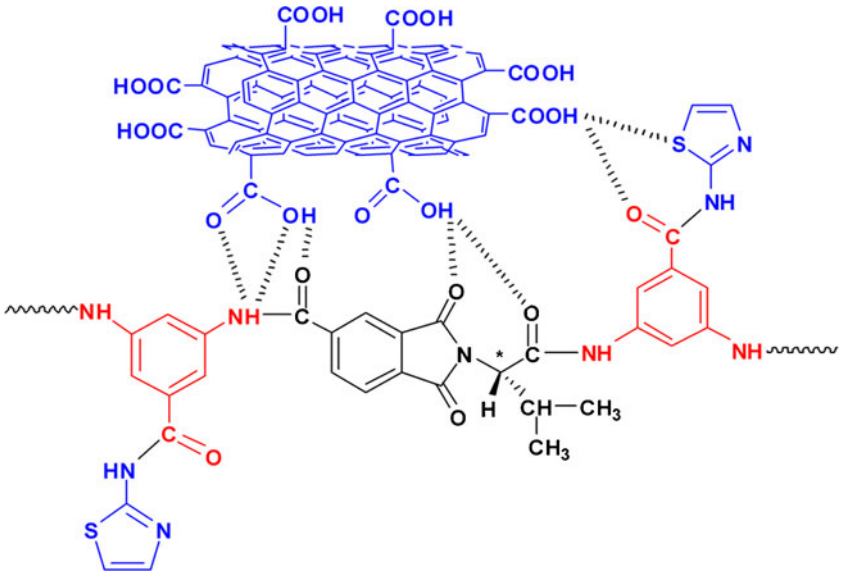

Fig. 1 Presentation possible interactions of hydrogen bonding between the MWCNT-COOH and the PAI chains

and 44° which are typically associated with the diffraction of metal impurities (2θ=26° corresponds to the (002) diffraction plane of the impurity graphite and 2θ=44° to α-Fe (110) and/or Ni (111) diffractions) [36]. For the neat PAI, the weak reflection centered at a 2θ value around 20° was characteristic of the amorphous polymer. For the MWCNT composite samples, they showed similar XRD patterns to the pure polymer samples when the MWCNT composition was 5 wt.%. For the MWCNT content higher than 5 wt.%, the MWCNT/PAI composites exhibit peaks of PAI and MWCNTs, as shown in Fig. 2(c, d). The reflections at 2θ=20° and 26° became slightly increased, when the MWCNT composition was increased to 15 wt.%.

Thermal stability of composites

TGA and DTG analysis at a rate of 10 °C/min in a nitrogen atmosphere were utilized to examine the thermal properties of the CNT/PAI composites. TGA results of PAI and their composites in nitrogen at heating rate of 10 °C/min are shown in Fig. 3. The thermal stability of the polymer and composites was studied on the basis of 5 and 10 % weight losses (T_5 and T_{10}) of the samples and the residue at 800 °C. The onset of decomposition temperature of the composites is higher than that of pure PAI, and it shifts toward higher temperatures as the amount of MWCNTs is increased. The T_{10} of pure PAI and the MWCNT/PAI composites with increasing amount of the MWCNTs such as 5, 10, and 15 wt.% are 402, 418, 440, and 462 °C, respectively. The T_{10} of the composite with 15 wt.% MWCNTs exhibits a T_{10} 60 °C higher than that of pure PAI. It is clear that the MWCNT/PAI materials improve thermal stability due to the incorporation of MWCNTs. The end temperature of decomposition is also retarded with increasing MWCNT content. The masses remaining at 800 °C are almost entirely due to the remaining CNTs and are consistent with initial CNT loading. The weight percent remaining after major degradation at 800 °C was higher for composites than for neat PAI. This indicates MWCNT reduces the degradation of PAI at high temperature as the effect was clearly seen in the curves. The results indicate that the addition of CNTs significantly increased the thermal stability of PAI in nitrogen as the effect was clearly seen in the curves.

Two fascinating relationships have been found between the limiting oxygen index (LOI) and the parameters of the combustion process: char yield or char residue (CR) and heat of combustion. LOI also called critical oxygen index or oxygen index (OI) and it is defined as the minimum fraction of oxygen in a mixture of oxygen and nitrogen that will just support combustion (after ignition). On the

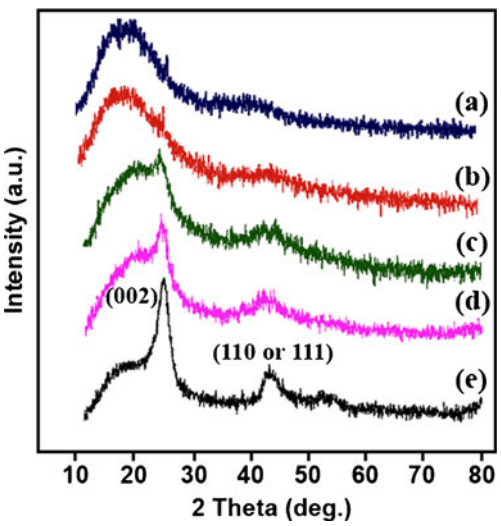

Fig. 2 Diffraction pattern data for MWCNT/PAI composite samples with different MWCNT contents: (*a*) 0 wt.%, (*b*) 5 wt.%, (*c*) 10 wt.%, (*d*) 15 wt.%, and (*e*) 100 wt.%

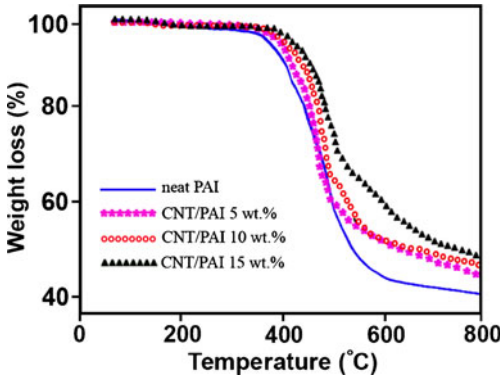

Fig. 3 TGA curves of the composites with different MWCNT loading under flowing nitrogen

other hand, OI methods describe the tendency of a material to sustain a flame.

According to Van Krevelen [37], there is a linear relationship between LOI and CR only for halogen-free polymers (Eq. 1):

$$\mathrm{LOI} = (17.5 + 0.4\mathrm{CR})/100 \tag{1}$$

According to this equation, a higher char yield will increase flame retardance. PAI and composites containing 5, 10, and 15 wt.% had LOI values 32.7, 34.7, 36.3, and 37.5, respectively, as calculated from their char yield. On the basis of the LOI values, such materials can be classified as self-extinguishing materials.

According to Johnson [38], the LOI values of many common materials can be logically well predicted by the expression (Eq. 2):

$$LOI = 8000/\Delta H_{comb} \tag{2}$$

where ΔH_{comb} is the specific heat of combustion in J/g. So, in the case of this polymer (PAI6) and MWCNT/PAI composites (5, 10, and 15 wt.%) ΔH_{comb} is 24.5, 23.0, 22.0, and 21.3 kJ/g, respectively.

Microscopy characterization

To characterize the morphology and dispersity of MWCNTs in the composites, FE-SEM images of fracture surfaces of neat nanostructured PAI and composites were examined as displayed in Fig. 4. The neat PAI copolymer showed a smooth fracture surface morphology (Fig. 4a). FE-SEM observation revealed that the PAI particles self-organized into nanopatterns. As can be seen from these images, the average diameter of polymeric particles is about 35 nm, and the shape of them is about spherical. For MWCNT/PAI composites, MWCNTs well dispersed and embedded in the PAI matrix without showing noticeable MWCNT aggregates (Fig. 4b–d). In addition, the fracture surface of MWCNT/PAI composites is relatively smooth without exhibiting the pull-out of MWCNTs from the PAI matrix and the boundary between MWCNT and PAI matrix is not discernible clearly. These results strongly support that due to hydrogen bonding between MWCNT-COOH and functional groups in the PAI matrix, the MWCNTs are wrapped around PAI nanoparticles and MWCNTs are also mixed well with

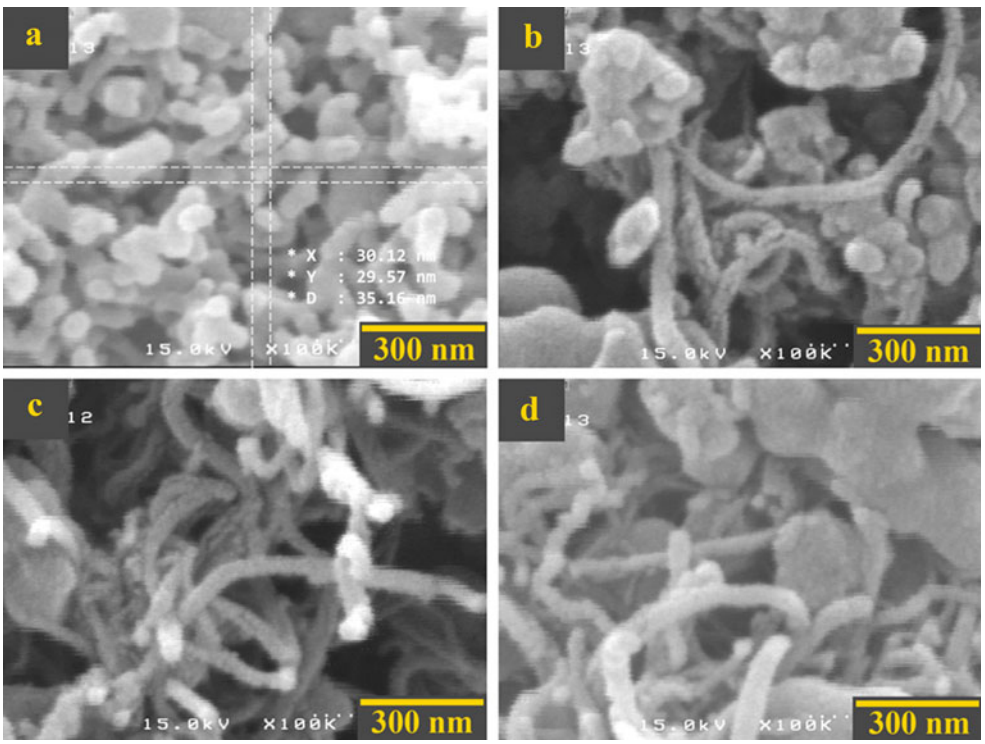

Fig. 4 Fracture surfaces of the produced materials: **a** pristine PAI and composites containing **b** 5 wt.%, **c** 10 wt.%, and **d** 15 wt.% MWCNTs

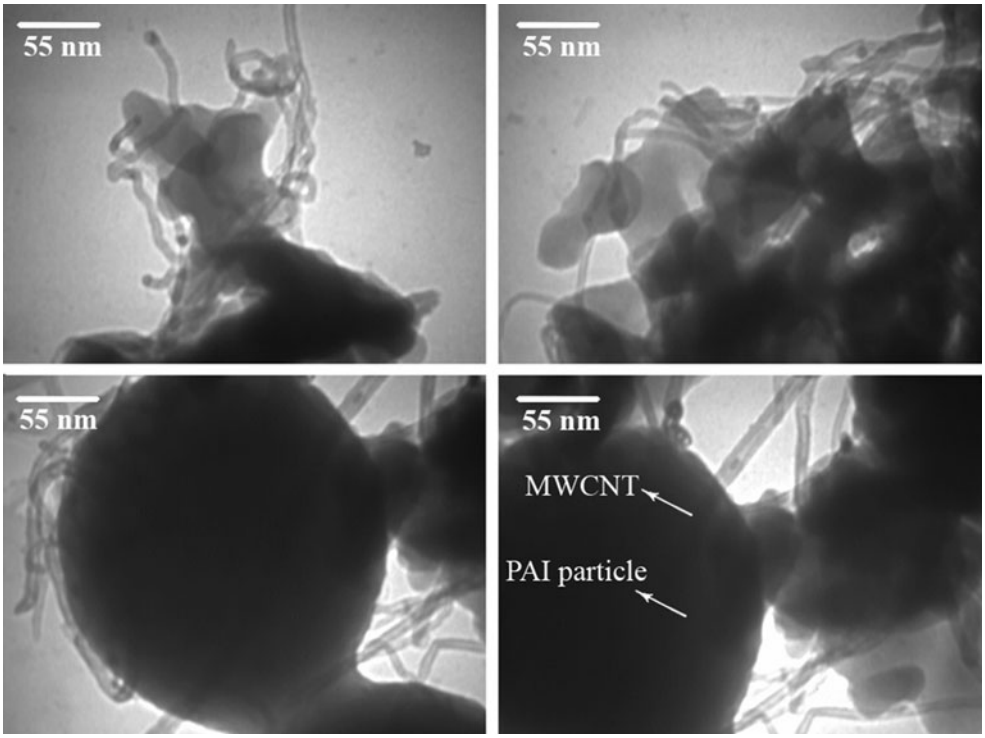

Fig. 5 TEM micrographs of MWCNTs/PAI composites containing 10 wt.% of CNT

the PAI matrix, eventually leading to the good dispersity of MWCNTs-COOH in the PAI matrix. The representative TEM images of the MWCNT/PAI composites are shown in Fig. 5. In general, the drawbacks related to the homogeneous dispersion of the CNTs in the polymer matrix resulted from intrinsic van der Waals attractions between the individual CNTs in combination with high aspect ratio and large surface area, making it difficult for the CNTs to disperse in the polymer matrix. The interfacial adhesion between the CNTs and the polymer matrix plays an important role in improving the dispersion of the CNTs into the polymer matrix. As shown in Fig. 5, the MWCNTs were dispersed well in the PAI matrix, which was explained by the fact that the MWCNT stabilizes their dispersion by good interactions with the PAI matrix, resulting from the increased polarity by the functional groups formed on the surfaces of MWCNTs as well as carbonyl groups in the PAI structure. The presence of the carboxyl groups on the surfaces of the MWCNTs resulted in the interfacial interaction between the polymer matrix and the CNTs in the composites. For example, a hydrogen bonding can be formed between the carboxyl groups at the MWCNT-COOH with the oxygen atoms at the carbonyl groups of the PAI as shown in Fig. 1.

Mechanical testing

It has been generally accepted that the nanoparticles or nanomaterials benefit the mechanical properties when they are well distributed in the polymer matrix [6]. In this study, MWCNTs-COOH were also found to greatly increase the mechanical properties of PAI due to the nanoreinforcing effect of CNT with high aspect ratio. The variations of mechanical properties of the MWCNT/PAI composites with CNT content are shown in Fig. 6. It can be seen that, in comparison with neat PAI film, the MWCNT/PAI composite films exhibit higher Young's modulus and tensile strength but smaller strain at break, and the strain at break decreases gradually with increasing MWCNT feeding content, while a significant increment in Young's modulus and a moderate increment in tensile strength are observed simultaneously. The Young's modulus and tensile strength increased from

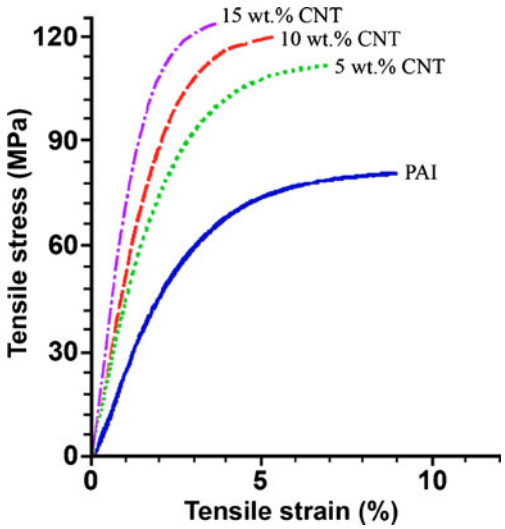

Fig. 6 Tensile stress–strain curves of MWCNT/PAI composites for concentrations ranging from 0 to 15 % MWCNTs by weight

1.9±0.1 GPa and 80.5±1.1 MPa for neat PAI film to 3.0±0.1 GPa and 112.4±1.3 MPa, 3.4±0.2 GPa and 120.7±1.2 MPa, and 3.5±0.1 GPa and 124.5±1.6 MPa for MWCNT/PAI composite films with increasing the MWCNT feeding content from 5 to 10 and 15 wt.%, respectively. Incorporation of 5 % MWCNTs into the PAI film increased its tensile strength to 60.4 MPa, which is about 32 % higher than that of the pure PAI counterpart. This increasing effect of CNT on the tensile strength and tensile modulus of composites was more significant at low CNT content when compared with high CNT content. The fact that the improvement in the mechanical properties of the composites was not increased at higher CNT content as expected, in comparison with that at low CNT content, was explained by the characteristics of CNT that tended to bundle together because of their intrinsic van der Waals attractions between the individual CNTs in combination with high aspect ratio and large surface area and could lead to some agglomeration, causing the stress concentration phenomenon and preventing efficient load transfer to the polymer matrix. In this study, the reinforcing efficiency of MWCNT-COOH is defined as the normalized mechanical properties of the composites with respect to those of pure PAI. The improvement of the mechanical properties of the MWCNT/PAI composites was attributed to the better interfacial bonding between the MWCNTs and the PAI matrix as well as the better dispersion of the MWCNT in the PAI matrix. The incorporation of the MWCNT-COOH and several functional groups into the PAI matrix resulted in the good interfacial adhesion between the MWCNT-COOH and the PAI matrix. This interaction between the MWCNT-COOH and the PAI matrix is crucial for improving the mechanical properties of the composites. The elongation at break of the composites decreased with the introduction of MWCNT, indicating that the composites became somewhat brittle when compared with pure PAI because of the increased stiffness of the composites and decreased mobility of PAI matrix. Such an embrittlement phenomenon has also been observed in other CNTs reinforced polymer systems [39, 40].

Conclusions

In summary, we demonstrated a straightforward procedure to prepare aromatic MWCNT/PAI composite films based on the nanostructured PAI and the MWCNTs-COOH for improving the dispersion and the interfacial adhesion by simple solution casting method using ultrasonication process. The addition of acid-modified MWCNTs into the PAI matrix led to obvious improvements in the thermal and mechanical properties. The significant improvements effects are due to the reinforcement of finely dispersed MWCNTs fillers throughout the matrix as well as the strong hydrogen interaction between carboxyl functional groups in the MWCNTs and carbonyl groups in the PAI matrix, thus being favorable to stress transfer from polymer to CNTs. Microscopic observations revealed that a more uniform and fine dispersion of the MWCNTs were achieved throughout the PAI matrix. Future improvement of this work may include better choices of concentration for different polymer materials, a more complete understanding of the interfacial chemistry and the mechanism of dispersion, optimization of CNT contents in the composite for different applications, and better understanding of the adhesion between the CNTs and the polymer matrix.

Acknowledgments The study is financially supported by Research Affairs Division Isfahan University of Technology (IUT). Further, financial support from National Elite Foundation and Center of Excellency in Sensors and Green Chemistry Research (IUT) is gratefully acknowledged.

References

1. Harris PJF (1999) Nanotubes and related structures—new materials for the twenty-first century. University of Cambridge Press
2. Baughman RH, Zakhidov AA, De Heer WA (2002) Carbon nanotubes—the route toward applications. Science 297:787–792
3. Alimohammadi F, Parvinzadeh Gashti M, Shamei A (2012) Functional cellulose fibers via polycarboxylic acid/carbon nanotube composite coating. J Coat Technol Res. doi:10.1007/s11998-012-9429-3
4. Du Y, Shen SZ, Yang WD, Chen S, Qin Z, Cai KF, Casey PS (2012) Facile preparation and characterization of poly(3-hexylthiophene)/multiwalled carbon nanotube thermoelectric composite films. J Electron Mater 41:1436–1441
5. Diez-Pascual AM, Naffakh M, Marco C, Ellis G (2012) Mechanical and electrical properties of carbon nanotube/poly(phenylene sulphide) composites incorporating polyetherimide and inorganic fullerene-like nanoparticles. Composites Part A 43:603–612
6. Kim SW, Kim T, Kim YS, Choi HS, Lim HJ, Yang SJ, Park CR (2012) Surface modifications for the effective dispersion of carbon nanotubes in solvents and polymers. Carbon 50:3–33
7. Bechinger C, Rudhardt D, Leiderer P, Roth R, Dietrich S (1999) Understanding depletion forces beyond entropy. Phys Rev Lett 83:3960–3963
8. Frank S, Poncharal P, Wang ZL, de Heer WA (1998) Carbon nanotube quantum resistors. Science 280:1744–1746
9. Karabanova LV, Whitby RLD, Bershtein VA, Korobeinyk AV, Yakushev PN, Bondaruk OM, Lloyd AW, Mikhalovsky SV (2012) The role of interfacial chemistry and interactions in the dynamics of thermosetting polyurethane–multiwalled carbon nanotube composites at low filler contents. Colloid Polym Sci. doi:10.1007/s00396-012-2745-4
10. Liu T, Xu G, Zhang J, Zhang H, Pang J (2012) Dispersion of carbon nanotubes by the branched block copolymer Tetronic 1107 in an alcohol–water solution. Colloid Polym Sci. doi:10.1007/s00396-012-2745-4
11. Hill D, Lin Y, Qu L, Kitaygorodskiy A, Connell JW, Allard LF, Sun YP (2005) Functionalization of carbon nanotubes with derivatized polyimide. Macromolecules 38:7670–7675

12. Chen GX, Kim HS, Park BH, Yoon JS (2005) Controlled functionalization of multiwalled carbon nanotubes with various molecular-weight poly(L-lactic acid). J Phys Chem B 109:22237–22243
13. Diez-Pascual AM, Naffakh M, Gomez MA, Marco C, Ellis G, Gonzalez-Dominguez JM, Anson A, Martinez MT, Martinez-Rubi Y, Simard B, Ashrafi B (2009) The influence of a compatibilizer on the thermal and dynamic mechanical properties of PEEK/carbon nanotube composites. Nanotechnology 20:315707
14. Hu CY, Xu YJ, Duo SW, Zhang RF, Li MS (2009) Non-covalent functionalization of carbon nanotubes with surfactants and polymers. J Chin Chem Soc 56:234–239
15. Liu L, Zheng Z, Gu C, Wang X (2010) The poly(urethane-ionic liquid)/multi-walled carbon nanotubes composites. Compos Sci Technol 70:1697–1703
16. Zhao JC, Du FP, Zhou XP, Cui W, Wang XM, Zhu H, Xie XL, Mai YM (2011) Thermal conductive and electrical properties of polyurethane/hyperbranched poly(urea-urethane)-grafted multi-walled carbon nanotube composites. Composites Part B 42:2111–2116
17. Xu J, Yao P, Jiang Z, Liu H, Li X, Liu L, Li M, Zheng Y (2012) Preparation, morphology, and properties of conducting polyaniline-grafted multiwalled carbon nanotubes/epoxy composites. J Appl Polym Sci 125:E334–E341
18. Jeon IY, Tan LS, Baek JB (2008) Nanocomposites derived from in situ grafting of linear and hyperbranched poly(ether-ketone)s containing flexible oxyethylene spacers onto the surface of multi-walled carbon nanotubes. J Polym Sci Polym Chem 46:3471–3481
19. Diez-Pascual AM, Martinez G, Martinez MT, Gomez MA (2010) Novel nanocomposites reinforced with hydroxylated poly(ether ether ketone)-grafted carbon nanotubes. J Mater Chem 20: 8247–8256
20. Cao L, Yang W, Yang J, Wang C, Fu S (2004) Hyperbranched poly (amidoamine)-modified multi-walled carbon nanotubes via grafting-from method. Chem Lett 33:490–491
21. Sun G, Chen G, Liu J, Yang J, Xie J, Liu Z, Li R, Li X (2009) A facile gemini surfactant-improved dispersion of carbon nanotubes in polystyrene. Polymer 50:5787–5793
22. Kim YS, Lee KH, Jung JC (1996) In: Mittal KL (ed) Polyimides and other high temperature polymers. Dekker, New York, pp 71–90
23. Koo M, Bae JS, Shim SE, Kim D, Nam DG, Lee JW, Lee GW, Yeum JH, Oh W (2010) Thermo-dependent characteristics of polyimide–graphene composites. Colloid Polym Sci. doi:10.1007/s00396-011-2469-x
24. Mallakpour S, Rafiee Z (2011) New developments in polymer science and technology using combination of ionic liquids and microwave irradiation. Prog Polym Sci 36:1754–1765
25. Yang CP, Su YY, Hsu MY (2006) Syntheses and properties of fluorinated polyamides and poly(amide imide)s based on 9,9-bis[4-(4-amino-2-trifluromethylphenoxy) phenyl]fluroene, aromatic dicarboxylic acids, and various monotrimellitimides and bistrimellitimides. Colloid Polym Sci 284:990–1000
26. Lee SH, Choi SH, Choi JI, Lee JR, Youn JR (2010) Rheological property and curing behavior of poly(amide-*co*-imide)/multi-walled carbon nanotube composites. Korean J Chem Eng 27:658–665
27. Lee SH, Choi SH, Kim SY, Young JR (2010) Effects of thermal imidization on mechanical properties of poly(amide-coimide)/multiwalled carbon nanotube composite films. J Appl Polym Sci 117:3170–3180
28. Lee SH, Choi SH, Kim SY, Choi JI, Lee JR, Youn JR (2010) Degradation and dynamic properties of poly(amide-co-imide)/carbon nanotube composite films. Polym Polym Compos 18:381–390
29. Lauwiner M, Rys P, Wissmann J (1998) Reduction of aromatic nitro compounds with hydrazine hydrate in the presence of an iron oxide hydroxide catalyst. I. The reduction of monosubstituted nitrobenzenes with hydrazine hydrate in the presence of ferrihydrite. Appl Catal A 172:141–148
30. Saeed S, Rashid N, Wong WT, Hussain R (2011) 3,5-Dinitro-N-(1,3-thiazol-2-yl)-benzamide monohydrate. Acta Cryst E67:o660. doi:10.1107/S1600536811005228
31. Mallakpour S, Ahmadizadegan H (2012) Poly(amide-imide)s obtained from 3,5-diamino-N-(thiazol-2-yl)-benzamide and dicarboxylic acids containing various amino acid units: Production, characterization and morphological investigation. High Perform Polym. doi:10.1177/0954008312459547
32. Mallakpour S, Hajipour AR, Shahmohammadi MH (2002) Novel optically active poly(amide-imide)s from N-trimellitylimido-S-valine and aromatic diamines by direct polycondensation reaction. Iran Polym J 11:425–431
33. Mallakpour S, Dinari M (2012) In: Mohammad A, Inamuddin (eds) Green solvents I: properties and applications of ionic liquids. Springer, Netherlands, pp 1–32
34. Mallakpour S, Rafiee Z (2012) In: Mohammad A, Inamuddin (eds) Green solvents II: Properties and applications in chemistry. Springer, Netherlands, pp 1–66
35. Lee HJ, Oh SJ, Choi JY, Kim JW, Han J, Tan LS, Baek JB (2005) In situ synthesis of poly(ethylene terephthalate) (PET) in ethylene glycol containing terephthalic acid and functionalized multiwalled carbon nanotubes (MWNTs) as an approach to MWNT/PET nanocomposites. Chem Mater 17:5057–5064
36. Pérez-Cabero M, Rodríguez-Ramos I, Guerrero-Ruíz A (2003) Characterization of carbon nanotubes and carbon nanofibers prepared by catalytic decomposition of acetylene in a fluidized bed reactor. J Catal 215:305–316
37. Van Krevelen DW (1975) Some basic aspects of flame resistance of polymeric materials. Polymer 16:615–620
38. Johnson PR (1974) A general correlation of the flammability of natural and synthetic polymers. J Appl Polym Sci 18:491–504
39. Siochi EJ, Working DC, Park C, Lillehei PT, Rouse JH, Topping CC, Bhattacharyya AR, Kumar S (2004) Melt processing of SWCNT-polyimide nanocomposite fibers. Composites Part B 35:439–446
40. Ge JJ, Zhang D, Li Q, Hou HQ, Graham MJ, Dai L, Harris FW, Cheng SZD (2005) Multiwalled carbon nanotubes with chemically grafted polyetherimides. J Am Chem Soc 127:9984–9985